

Dispersion from Courtyards and Other Enclosed Spaces

AIVC 11760

D.J. Hall, S. Walker, A.M. Spanton.

Building Research Establishment Ltd.
Garston, Watford, Herts WD2 7JR, UK

Abstract.

The paper describes small scale wind tunnel experiments on the dispersion of contaminants discharged from the bottom of courtyards and other enclosed spaces. The experiments covered a range of courtyards with ratios of depth to width from 5 (consistent with light wells and other very deep cavities) down to 0.1 (consistent with shallow enclosed squares and piazzas that are frequently found in the urban environment). A variety of parameters within these shapes were investigated, including the depth of the walls around the courtyard, the presence of openings in the walls, the effects of wind direction, the presence of surface clutter and stratification of the air in the courtyard. In general courtyards are poorly ventilating spaces and high residual concentrations of any discharged contaminant occur. However, this behaviour may also be used to advantage in using courtyards as a method of modifying the local climate. The effects of the parameters investigated on contaminant concentrations were complex and quite variable, which allows for the possibility of designing courtyards to suit specific needs.

Keywords: Pollution, Dispersion, Courtyards, Enclosed Spaces, Environmental Control

Notation.

- A H_{\max} / W , Aspect ratio of courtyard.
- A_d Area Density. Proportion of ground surface covered by obstacles.
- C Mean concentration of tracer.
- d Surface displacement, appearing in the usual rough wall velocity profile equation.
- D Thickness of courtyard walls (see Figure 3).
- F Buoyancy flux. Equations 4 and 5.
- g Acceleration due to gravity.
- H Height above ground.
- H_{\max} Maximum height of courtyard, also used as reference height for windspeed.

- K Dimensionless mean concentration, Equation 2.
- q Upward heat flux from surface or heat loss due to evaporative cooling.
- Q Rate of discharge of tracer. Equation 2.
- S Stratification parameter, Equation 6.
- U Windspeed.
- u' Longitudinal turbulence intensity.
- U_{ref} Windspeed at height H_{max} , the height of the courtyard. .
- U_* Friction velocity.
- V Volume flow rate of fluid in definition of buoyancy flux, F in Equation 4.
- W Width of courtyard (courtyards were square in the present experiments).
- z_0 Aerodynamic roughness length, appearing in the usual rough wall velocity profile equation,

$$\frac{U}{U_*} = \frac{1}{\kappa} \ln \left(\frac{z-d}{z_0} \right). \quad (1)$$

- ρ_a Ambient fluid density.
- $\Delta\rho$ Fluid density difference from ambient.

1. Introduction.

Courtyards are a common architectural form. They are used for the generation of private spaces, improving the ingress of light and control of the local microclimate at almost all latitudes. In Northern climates they are used as wind shelters and sun-traps and in Southern climates for shelter from the sun and the reduction of mean temperatures, for example by the evaporation of water. If the definition of ‘courtyard’ is expanded somewhat to take in other enclosed spaces it can include deep light wells and relatively shallow piazzas, largely enclosed squares and the private spaces (usually gardens) formed by outward-facing buildings set in squares. On this basis the enclosed square, courtyard or light well must be one of the most common features of the built environment. They are described here under the generic term of ‘courtyard’.

Despite this ubiquity, there seem to have been few investigations of the ventilation of courtyards and enclosed spaces generally. An interrogation of the 9000 plus papers and reports in the AIVC database yielded only about a dozen references. There were some descriptions of the use of courtyards for generating modified microclimates, for example Ahlemiddi(1991) and Al Azzawi(1991). There was also some work on the

ventilation of courtyards. For example Bensalem and Sharples(1989) measured ventilation rates of courtyards and atria using small orifice plate devices and Walker et al(1993) and Shao et al(1993) investigated the use of CFD for determining ventilation rates and used smoke for determining the clearance rates of contaminants in wind tunnel model and full scale courtyards.

The two main concerns in courtyard ventilation are, firstly, the direct rate of ventilation in terms of the removal of unwanted contaminants and, secondly, the generation and retention of a microclimate. The requirements are, of course, opposites, one requiring a maximised rate of dispersion of any discharged contaminants, the other preferring a minimum. There appeared, however, to have been no direct measurements of the ventilation of courtyards, or its equivalent, the dispersion of discharged contaminants from within them.

The present paper describes some direct measurements of dispersion from courtyards, using trace gases in small scale wind tunnel models. There are a large number of variables of interest and it has not been possible to investigate all of them thoroughly here. However the work presented here covers enough of these in sufficient detail to reveal the essential character of courtyard ventilation.

2. Details of Experiments

The description of the experimental procedures have been kept relatively brief here. A more detailed discussion can be found in Hall et al(1995).

The experiments were carried out in the BRE dispersion modelling wind tunnel at its Cardington laboratory. A diagram of the wind tunnel is shown in Figure 1. The working section is 22m long by 4.3m wide and 1.5m high. The forward part of the wind tunnel is used to generate a thick rough wall boundary layer, using a mixture of Counihan's(1969) turbulence generators plus a long fetch of rough surface. In the present experiments the boundary layer was grown over an array of 10mm square by 20mm high roughness elements on a 50mm spacing, to produce a roughness length, z_0 , for the boundary layer of about 2mm. A velocity and longitudinal turbulence intensity profile for the undisturbed boundary layer (measured with a pulsed wire anemometer) is shown in Figure 2, it had a depth of about 1m. Most of the experiments were carried out with a windspeed of 1.5ms^{-1} at 100mm height, but some involving stratified flows used windspeeds down to 0.3ms^{-1} in order to obtain the required levels of stratification.

The notation and terminology for the courtyards is given in Figure 3, which shows a 'folded out' diagram of the inner walls. The 'courtyards' were constructed from blocks of 100x100mm plan section in a range of heights from 10mm to 100mm. The blocks were close fitting when stacked together, so that there was no significant leakage between them. A diagram of a typical courtyard layout in the wind tunnel is shown in Figure 4. The courtyards were always of square planform, but varying depth, the ratio of height to width (H_{max}/W , defined here as the courtyard aspect ratio, A) ranging between 0.1 and 5. It was not possible to achieve this range of aspect ratios with a single planform size between the constraints of remaining well within the wind tunnel boundary layer and having an acceptable minimum depth for practical purposes. Two courtyard plan dimensions were therefore used, of 100mm x

100mm for the deeper courtyards, up to 500mm depth, and 200mm x 200mm for the shallower courtyards down to 20mm depth. Overlapping experiments with the same aspect ratio in both courtyard sizes, to be described later, showed no significant differences in their behaviour. The thickness of the walls surrounding the courtyard, D , was normally 100mm or 200mm, giving a value of D/W of 1.0. However some experiments investigated higher values of D/W .

Dispersion measurements were made using a diluted methane tracer (of 2.5% in air, with nearly neutral buoyancy) discharged uniformly through the floor of the courtyard at a fixed rate, as in Figure 4. Typical tracer discharge rates were low, about 0.1 l m^{-1} , so that the efflux velocity from the courtyard floor did not directly affect the airflow in the courtyard. The dispersed tracer was sampled through 1mm bore tubing to a flame ionisation detector system (FID) which was specially designed for this type of work. It uses three FID's running through selector valves so that a large number of sampling points can be used. A fourth FID constantly monitors the background level of tracer so that this can be subtracted from the measurement in progress. Sample averaging times were of two minutes duration, sufficient to give a stable mean concentration. Experiments are quality controlled by a number of cross checks, including a mass balance measurement on a free plume for which the tracer emission rate and the integrated flux of concentration should agree, which checks out the whole system. Agreement was within 5.5% in the present experiments. Also the first measurement of each test uses the same sampling point for all three FID's, which must agree. Overall accuracy of measurement of trace gas concentration is about 10%. The system is more fully described in Hall et al(1995).

Trace gas concentrations were measured at about 20 sampling points (the number depending upon the depth of the courtyard). One measurement was set in the centre of the courtyard floor, on a metal disc of 20mm diameter and the remainder up the midlines of the inside walls and on the roof of the courtyard.. A typical sampling layout is also shown in Figure 4. All concentration measurements were non-dimensionalised in the usual form of a dimensionless concentration, K , defined here as,

$$K = \frac{CU_{ref}W^2}{Q} \quad (2)$$

Given a value of K for the experiment, the concentrations of contaminants at full scale can be determined by providing appropriate values of the other variables.

In the experiments with stratified flow in the courtyards, either buoyant or heavier-than-air gases were added to the trace gas to generate unstable or stable stratifications. This is discussed in more detail in Section 4.4, which deals with these cases.

Equation 2 is that usually used to define the dimensionless concentration, K , based on dispersed contaminant concentration, C , from a release at a discharge rate Q . However, the other interest in the dispersion characteristics of courtyards noted in the introduction is related to the dispersion of heat and its effect on the air temperature in

the courtyard. In this latter context, Sanchez and Alvarez (1997) have noted that the analogy of Equation 2 for this purpose is,

$$K = \frac{\rho_a C_p (T - T_a) U_{ref} W^2}{q} \quad (3)$$

Thus values of K obtained from the dispersion of tracers (as in the present experiment) can be used to predict the temperature rise, $T - T_a$, due to a heat flux q .

3. Velocity Profiles Through Courtyards.

Velocity profile measurements were made up through the centre of the basic courtyards using a pulsed wire anemometer. This records both positive and negative velocities and also produces a reliable measurement of longitudinal turbulence intensity through the recirculating flow in the courtyard where reversed flow occurs. The results of the measurements are shown in Figure 5, for courtyards set square to the wind. The profiles fell naturally into three groups, which are plotted separately. These were, shallow courtyards with low aspect ratios ($A = H_{max}/W = 0.1$ and 0.2 , the top plot), courtyards with intermediate aspect ratios ($0.3-1.0$, the centre plot) and deep courtyards with high aspect ratios ($1-5$, the bottom plot). Both mean velocity (the left hand profile) and longitudinal turbulence intensity (the right hand profile) are shown. All heights are scaled relative to the courtyard depth, H_{max} , and velocities and turbulence intensities are scaled relative to the undisturbed windspeed, U_{ref} , at height H_{max} .

The two low aspect ratio courtyards, in the upper plot, showed mean velocity profiles with reduced velocities near the ground but little or no reversed flow. The mean velocity profiles for the intermediate depth courtyards, in the centre plot, all collapsed on to the same curve, with negative velocities near the ground becoming steadily more positive up through the courtyard into the free stream. There was a sharp change in the profile gradient at the edge of the free shear layer over the top of the courtyard, above which the velocity remained nearly uniform. The deep courtyards, in the bottom plot, showed nearly zero or slightly negative mean velocities up through the courtyard until the region close to its opening when the mean velocity became negative and then sharply positive out through the top of the courtyard. Above the free shear layer the velocity was then almost uniform.

The turbulence intensities in Figure 5 showed high levels for the shallow courtyards and levels that increased with height for the intermediate and deep courtyards. In the latter cases the maximum turbulence intensities occurred just above the courtyard opening at the edge of the shear layer. For each of the three courtyard groups, the turbulence intensity profiles showed similar forms but did not collapse on to single curves as with the mean velocities.

The mean velocity profiles for the three courtyard groups result from the different wind recirculation patterns within the courtyards in these cases. These are sketched (not to scale) in Figure 6. In the shallow courtyards there was limited or no recirculation. The free shear layer over the courtyard spread back towards the surface and either re-attached to the ground or came close to doing so. In the intermediate

depth courtyards there was a strong recirculating eddy in the courtyard cavity which penetrated to its base, thus there was a continuous velocity gradient up through the courtyard, passing through zero (the centre of the recirculating eddy) at about half the courtyard height. In the deep courtyard there was also a recirculating eddy, but it remained approximately circular in cross section and thus did not penetrate to the bottom of the courtyard, leaving a slow moving, unsteady airflow pattern close to the ground. Thus the region of negative velocity and positive velocity gradient consistent with the recirculation pattern was at the top of the courtyard opening in these cases.

4. Dispersion Measurements in Courtyards.

4.1. The Behaviour of Closed Empty Courtyards of Varying Aspect Ratio.

Figure 7 shows vertical concentration profiles up the centrelines of the walls of courtyards of varying aspect ratio set normally to the wind. The plot shows all the courtyard aspect ratios used, with the shallower courtyards in the upper plots and the deeper courtyards in the lower plots. The three plots of each pair show the concentrations respectively on the upwind wall, downwind wall and the two side walls. Note that the concentration scale covers five decades. All the plots for different walls and aspect ratios showed similar behaviour, of a generally reducing concentration with increasing height, though the concentration gradients varied with wall position and aspect ratio. There was generally a steeper gradient of concentration at the upper levels of the courtyards and a very sharp gradient across the roof of the structure, except on the downwind side, where the concentration remained relatively steady. Typically, concentrations in the courtyards fell by an order of magnitude or more from the bottom to close to the top. The proportionate reduction was about the same irrespective of the aspect ratio of the courtyard, so that the gradients reduced as the aspect ratio increased.

All the data plots of this sort showed similar behaviour for nearly all the courtyard parameters investigated. It was concluded from this that the vertical gradients of concentration were sufficiently well ordered for the concentration at the base of the courtyard to be a good indicator of the concentrations elsewhere within it. This single measurement has therefore been used extensively in the results presented here.

Concentrations at the base of courtyards of varying depth, that is those in Figure 7, are shown in Figure 8, plotted against aspect ratio for courtyards normal to the wind. Two sets of data are shown for the two scales of the experiment. In the region of overlap of they are quite similar. The plot shows a curious behaviour, with a maximum in concentration at the base of the courtyard for an aspect ratio of 0.3 and a minimum at an aspect ratio of about 1.5. For deeper courtyards, concentrations increased steadily to high values with increasing aspect ratio. This behaviour is related to the recirculation pattern in the courtyard cavity, it is considered more fully in the discussion in Section 5.

The effects of wind direction on the courtyard concentrations are shown in Figure 9, which gives the concentration at the base as a function of wind direction for three aspect ratios, 0.3, 1.0 and 3.0. These correspond to the aspect ratios giving concentrations at the maximum, minimum and some way up the rising levels for deep courtyards in Figure 8. A wind direction of 0° corresponds to a flow normal to the upwind face of the courtyard and data are given around to 45° , the point of symmetry.

For the lowest aspect ratio, of 0.3, the effects of wind direction were relatively slight, with concentrations reducing by about 20% around to 45° wind direction. For the aspect ratio of 1.0, the concentration approximately doubled for wind directions around to 15°, beyond which it remained roughly constant. However, for the deeper aspect ratio the concentration remained roughly constant for wind directions around to 15°, beyond which the concentration fell by about a factor of three to a minimum at 30°, before rising again round to 45°, where the concentration was about two thirds of its value at 0°.

The effects of wall thickness on courtyard concentration are shown in Figure 10, which covers wall thickness ratios, D/W from the basic value of the experiments, 1.0, up to 5.0. Results are given for two aspect ratios, 0.3 and 1.0. In both cases increasing the wall thickness uniformly increased concentrations in the courtyard. For the lower aspect ratio, of 0.3, concentrations increased by about 30% up to the greatest wall thickness. The larger aspect ratio, of 1.0, showed a much greater increase in concentration, by about a factor of five, over this range of wall thickness.

Figure 11 shows vertical concentration profiles up the courtyard wall centrelines for the results of Figures 9 and 10, for varying wind direction and wall thickness. As with the vertical concentration profiles of Figure 7, for varying aspect ratio, there was mainly a well ordered concentration gradient, with concentration reducing steadily with increasing height.

4.2. Courtyards with Openings.

A common feature of courtyards and enclosed spaces is the presence of openings in the walls. Two types of opening, shown in Figure 12, have been investigated here. The first was an archway or tunnel entrance at the ground, which was of square cross section and size $W/2$. The second was an opening in a corner up the whole of one wall, of width $W/4$. The first type of opening is a common form of entrance to courtyards. The second type of opening was intended to represent an access street to an otherwise enclosed square. There are often, of course, several of these, but in the first instance a single opening of this type was investigated. A single courtyard aspect ratio, of 1.0, was used.

Figure 13 shows concentrations at the base of the courtyard for the two types of opening and a range of wind directions round to 180°, the point of symmetry. A wind direction of 0° corresponds to the opening facing into the wind. Data for a closed courtyard, with no openings, are shown for comparison. The concentrations show a complex behaviour with varying wind direction. With an archway opening, concentrations were generally below those of the closed courtyard by a factor of two to three, except in the 90° and 180° wind directions, when they were greater. With a corner opening facing into the wind there was a considerable increase in concentration in the courtyard, by a factor of three or more. However, as the wind direction passed 90° (with the opening along the wind), concentrations fell well below those for a closed courtyard, again by about a factor of three. Then, as the wind direction approached 180° (with the opening facing downwind), concentrations rose again to a level above that for the closed courtyard.

4.3. The Effects of Ground Clutter.

It is common to find substantial amounts of ground clutter in courtyards and other enclosed spaces, both solid obstacles and those porous to airflows like foliage. The effects of this were investigated using the two types of model 'clutter' shown in Figure 14. These were surface mounted obstacles in the form of cylinders of about twice height to diameter, solid or porous. The porous obstacles were of gauze with a 2mm mesh and an open area of about 50%, mainly intended to simulate trees and bushes. The obstacles were placed with an even spacing covering a range of area densities (the proportion of the surface area covered by obstacles) from 12% to 48%. The central space of the courtyard floor, where the single sampling point lay, was left clear, as in the example plan layout in Figure 14. Measurements were made for two courtyard aspect ratios, 0.3 and 1.0, constructed at the larger experimental size of 200mm square. Thus the clutter occupied 25% of the height of the deeper courtyard and 83% of the height of the lower courtyard.

The effect of surface obstacles on concentrations on the floor of the courtyard is shown in Figure 15, for both solid and porous obstacles, as a function of the area density of the obstacles. For both courtyard aspect ratios, an increasing area density of obstacles generally produced an increase in concentrations at the ground. The behaviour was similar for both solid and porous obstacles, but porous obstacles usually produced the greatest proportionate increase in concentration. The greatest difference was in the effects of the obstacles on the two courtyard depths. The lower courtyard, for which the obstacles occupied nearly the whole depth, showed only a limited increase in concentration at its base over the range of occupational densities of around 50%. However, for the deeper courtyard, for which the obstacles occupied 25% of the total depth, the concentration at the courtyard base increased by about a factor of 8 over the range of area densities, the most marked change occurring for area densities beyond 20%.

4.4. The Effects of Surface Stratification.

It is readily possible for the surfaces of courtyards to become cooler or warmer than the surrounding air and, as a result, to generate stable or unstable stratification in the air near the ground. This may occur naturally, or by design if deliberate attempts are made at climate modification in the courtyard. One common example of this is using the evaporation of water for cooling.

It must be appreciated that it is not temperature differences per se that maintain the stratification, but the continuous transfer of heat, either into or out of the ground or by evaporative cooling, to the surrounding air, without which any stratification would collapse rapidly. The critical parameter for scaling the stratification is the dimensionless buoyancy flux parameter, the usual form of which is,

$$\frac{F}{U^3 L} \quad (4)$$

Here, U is a windspeed and

L is a characteristic length scale of the flow, taken here as W.

F is a flux of buoyancy, which is expressed either as the introduction of fluid of different density into the flow (as in a hot plume, for example) or as an equivalent transfer of heat. Thus in the first definition,

$$F = g \frac{V}{\pi} \frac{\Delta\rho}{\rho}, \quad (5)$$

where V is a volume rate of flow of a gas of density difference $\Delta\rho$ from the surrounding fluid, of density ρ . g is acceleration due to gravity. It can also be shown that F can be defined in terms of a heat flux to the ground, Q, in the form,

$$F = 8.96Q. \quad (6)$$

where Q is then in units of MW.

This form of scaling is commonly used to model buoyant discharges in small scale wind tunnel models. A fuller consideration can be found in Hall et al(1995).

The larger the value of the buoyancy flux parameter, Equation 3, the greater will be any effects of stratification. It can be seen that its value is very sensitive to windspeed, diminishing rapidly as the windspeed increases. Thus strong stratification is mainly a phenomenon associated with low windspeed. With their generally low internal windspeeds, courtyards should have a significant potential for generating stratification.

In the present case the buoyancy flux can be either the upward heat flux from the ground (either positive for unstable stratification or negative for stable) or an equivalent heat flux from the evaporation of water where this is used deliberately for climate modification. Since the surface heat flux is normally measured in Watts m^{-2} , a suitable dimensionless form of the buoyancy flux parameter, called here the stratification parameter, S, for stratification in courtyards would be,

$$S = 8.96 \cdot 10^{-6} \cdot \frac{qW}{U_{ref}^3}, \quad (7)$$

where q is the surface heat flux in Watts m^{-2} (positive for outward heat flux and unstable stratification and negative for inward heat flux and stable stratification), W is the side length of the courtyard as previously and U_{ref} is the windspeed as previously.

For normal atmospheric surface heat transfer, in the UK values of q range between about +250 Watts m^{-2} and -30 Watts m^{-2} (Clarke(1979), Figure 4). If q is generated by the evaporation of water near the ground, the evaporation of 1 g s^{-1} of water per m^2 of ground surface area gives rise to a value of q of 2257 W m^{-2} , so that the evaporation of quite small amounts of water will generate the equivalent of significant stabilising heat fluxes.

Particular values of the stratification parameter, S , will produce specific flow and dispersion patterns. Figure 16 shows the values of S produced by different combinations of windspeed, courtyard size and surface heat flux. It is given as a plot of the values of S obtained for the product of courtyard size, W , and surface heat flux, q (in Watts m^{-2}), described on the plot as a 'dimensional heat flux', against windspeed. The plot is valid for both negative and positive values of q , except of course that the sign of S is reversed when q is negative.

The wind tunnel experiments simulated the heat transfer by directly injecting dense or buoyant gas (argon or helium) through the porous base of the courtyard, along with the trace gas. This produces a flux of buoyancy, which is equivalent to a surface heat transfer or ground-based evaporative cooling as discussed above. Further details of this principle can be found in Hall et al(1995). As was noted above, the value of S , depends upon the windspeed as well as the buoyancy flux and courtyard scale. In order to obtain the larger values of S while keeping the buoyant gas discharge within acceptable limits, it was necessary to reduce the wind tunnel windspeeds, down to $0.35m\ s^{-1}$ in the most extreme cases. This is a normal procedure in this type of wind tunnel experiment. Due consideration is given to maintaining adequate Reynolds numbers in this type of experiment, though it is often necessary to strike a balance with the need to obtain the required buoyancy fluxes. Hall et al(1995) consider this in more detail.

Figure 17 shows vertical profiles of concentration up the centres of the courtyard walls for a range of values of the stratification parameter, S . Results are shown for two courtyard aspect ratios, 0.3 and 1.0 and normal wind directions (0°). With one exception, the vertical concentration gradients show no particular differences over those for other experiments presented here, being fairly well ordered and showing monotonic gradients. The single exception is the downwind wall for the lower courtyard aspect ratio, of 0.3, where the vertical gradient was much more pronounced and concentrations fell to zero before the top of the courtyard. It appears that the stratification (both stable and unstable) had some effect on the air circulation pattern within the courtyard, allowing external air to penetrate more deeply down the downwind face of the courtyard than was normally the case.

Figure 18 shows concentrations at the base of the courtyard as a function of the stratification factor, S , for the two aspect ratios. A value of S of zero is neutrally stratified, as has been all the data presented so far. The ranges of S for stable and unstable stratification are based on estimates related to the different maximum surface heat fluxes which occur in the atmosphere. Maximum negative heat fluxes, from solar radiation, are about an order of magnitude greater than positive heat fluxes, which are largely due to conduction at the surface unless the evaporation of water is involved.

The courtyards for both aspect ratios showed similar behaviour with stratification. With increasingly positive values of S (unstable stratification) concentrations at the base of the courtyard fell and with increasingly negative values of S (stable stratification) concentrations rose, at least initially. Small amounts of stratification caused quite large changes in concentration at the ground. With unstable stratification concentrations fell steadily as the level of stratification increased. With stable stratification, however, concentrations increased to a high maximum at values of S

around -0.002, before falling rapidly for further decreases in S . The reason for this behaviour is not clear. The courtyards for both aspect ratios showed this general behaviour, the only difference between them being that the effects of stratification were more marked for the deeper courtyard.

From these limited experiments it appears that stratification is an important feature in dispersion from courtyards. The range of concentrations at the base of the courtyards over the range of stratification covered here was about 10:1 for the shallow courtyard, of aspect ratio 0.3, and about 200:1 for the deeper courtyard, of aspect ratio 1.0.

5. Discussion.

The first point that must be made in the light of the present work is that courtyards are generally very poorly ventilating places. The values of the dimensionless concentration, K , measured here at the base of the courtyards ranged from a low of about 5 to a high approaching 300. Typical values were around 50-200. In comparison with the relatively large number of dispersion measurements of contaminant concentration around the outside of rectangular buildings (see, for example, the reviews of Hosker(1980) and Hall et al(1996a)), if there is complete entrainment of the contaminant in the building wake, values of K immediately downwind in the wake would be of order unity. With the definition of K used here, based on the width of the courtyard rather than the overall width of the building, a typical value of K ought to be about 0.5. During the course of the experiment, in view of the very high values of K being obtained in the courtyards, we made such a measurement and obtained a value of K of 0.6, close to what would be expected.

From the point of view of the dispersion of contaminants, this seems a serious matter and it is clearly desirable to avoid the discharge or entrainment of contaminants into courtyards. For example, it would appear that a single motor vehicle exhaust discharging in a courtyard (large courtyards are commonly used as car parks) would produce contaminant levels on a par with about one hundred vehicle exhausts discharging just outside the building.

As far as the opposite interest is concerned, courtyards do indeed seem to be very good places in which to try and generate a microclimate and their use for this purpose appears to be technically well founded. In view of the profound effects of even modest levels of stratification, the use of evaporating water to provide both cooling and to stably stratify the atmosphere in courtyards to assist retaining the generated microclimate seems to have a sound physical basis. The use of distributed surface obstacles, whether foliage or solid, also seems to be a useful method of assisting retention of microclimates.

It also appears from the experiments here that rates of dispersion from courtyards are sensitive to most of the variables investigated, in some cases showing order of magnitude variations. This is useful from the architect's and designer's point of view, as the judicious choice of design parameters can be used to modify courtyard ventilation rates either upwards or downwards as desired. Though most of the design parameters of interest have been investigated here at least briefly, there are some other items which would also merit attention. These are the effects of courtyard plan shapes and the effects of variable wall heights around courtyards. Both are common features

of real courtyards and there is good reason to suppose that rates of dispersion will also be sensitive to them. It is also likely that the surrounding structures will affect courtyard ventilation by modifying flow patterns at the top of the courtyard. The effects of increasing wall thickness investigated here is probably a good indicator of the effects that might be expected.

The character of dispersion from Courtyards is intimately bound up with the behaviour of the wind-driven recirculating vortex in the courtyard space, some of which has been described in Section 3 and shown sketched approximately in Figure 6. Modifications to the courtyard shape and character which diminish or intensify this vortex equally result in matching increases and decreases respectively in the rates of dispersion. Thus the apparently curious results of Figure 8, which show the effects of aspect ratio on dispersion, can be explained in these terms. In general, the recirculating vortex prefers to be circular in cross section and in this state it appears to have the greatest intensity. If the space in which it is contained is far from this form then its intensity is diminished in some way. Thus in Figure 8, the minimum concentration in the courtyard occurred when its aspect ratio was approximately unity and the recirculation could be circular in cross section and fill the courtyard. As the courtyard depth increased beyond this, the recirculation remained of circular cross section, but remained at the top the courtyard, leaving a low velocity region with low rates of dispersion at the base of the courtyard. When the courtyard depth reduced below unity aspect ratio, the recirculating vortex was deformed out of its preferred form and the velocities and resultant rates of dispersion diminished. As a result, concentrations in the base of the courtyard continued to rise as the aspect ratio fell until the courtyard was shallow enough for the separated shear layer over its opening to re-attach back at the ground within the courtyard. This occurred with aspect ratios below 0.3 and the resultant increased rate of dispersion explains the maximum in the concentration at this point.

This phenomenon has also been observed by the first author in other work on the flows in closed containers, which have quite similar aerodynamic properties to courtyards. In an investigation of the water retention properties of cylindrical rain gauges of varying depth (Hall et al(1993)), a measurement of the windspeed required to remove droplets and snowflakes from the gauge produced a very similar plot to that of Figure 8 for essentially the same reasons. That is, the highest velocities in the base of the gauge (and the most rapid removal of its content) were associated with aspect ratios close to unity.

In a similar way, the presence of openings sometimes increased and sometimes decreased concentrations in the courtyards, though it might be expected in principle that any additional form of ventilation of the courtyard space ought to reduce concentrations. This is again related to the effects of the additional cross flows in the courtyards sometimes diminishing and sometimes re-inforcing the recirculating vortex.

6. Conclusions.

Measurements of dispersion from courtyards have shown that these are quite poorly ventilating spaces with resultant high concentrations of contaminants discharged at the base of the courtyard. Values of the dimensionless concentration, K , at the base of the

courtyards ranged between 5 and 300, with typical values between 50 and 200. These values are orders of magnitude higher than levels around the exteriors of buildings from locally discharged contaminants, which are typically of order unity.

This is disadvantageous for removing contaminants, but advantageous in generating desired microclimates within courtyards, for example stabilisation and cooling of the local atmosphere using evaporated water.

A wide of courtyard parameters have been investigated, aspect ratio, wind direction, wall thickness, the presence of openings and surface clutter and the generation of stratification by heating or cooling the base of the courtyard. All had significant effects on concentrations within the courtyards, often altering them by orders of magnitude. An implication of this is that there is good potential for designing courtyards for high or low rates of ventilation, as desired, by the judicious choice of the relevant design parameters.

7. Acknowledgements.

The work described here was part of the POLIS Project (on integrated urban planning) in the EC JOULE 95 research programme under contract No. JOR3-CT95-0024. It was co-funded by the European Commission (DG XII/F) and by the Construction Directorate of the UK Department of Environment, Transport and the Regions.

The authors are indebted to their colleagues on the POLIS project, and in particular to Professor Servando Alvarez of the University of Seville, for many interesting discussions on this topic and for introducing them to the concept of using courtyards to generate microclimates.

8. References

Alhemiddi N.A.(1991). Preliminary Investigation of the Effect of a Passive Direct Evaporative Cooling System on a Courtyard at UCLA.

‘Architecture and Urban Space’. 9th International Conference PLEA, Seville, Spain, Sept 24-27th, 1991. pp643-652. Kluwer Academic Publishers.

Al Azzawi S.(1991). Not Every Courtyard is Necessarily a Good One Climatically: Physical Characteristics Design of Domestic Courtyards in the Hot-Dry Climates of the Sub-Tropics.

‘Architecture and Urban Space’. 9th International Conference PLEA, Seville, Spain, Sept 24-27th, 1991. pp287-298. Kluwer Academic Publishers.

Bensalem R., Sharples S.(1989). Natural Ventilation in Courtyard and Atrium buildings.

The European Conference on Architecture. 4-8th December, Paris, France.

Clarke(1979). A Model for Short and Medium Range Dispersion of Radionuclides Released to the Atmosphere.

National Radiological Protection Board, Report No NRPB R91.

Counihan J.(1969). An Improved Method of Simulating an Atmospheric boundary Layer in a Wind Tunnel.

Atmospheric Environment. Vol. 3, pp197-214.

Hall D.J., Irwin J.G., Stone B.H., Upton S.L.(1993). Aerodynamic Considerations in Precipitation Collector Design.

Measurement of Airborne Pollutants (Ed. Couling). Butterworth-Heinemann, ISBN 0 7506 0885 4

Hall D.J., Kukadia V., Walker S., Marsland G. W.(1995). Plume Dispersion from Chemical Warehouse Fires.

Building Research Establishment, Report No. CR56/95.

Hall D.J., Spanton A.M., Macdonald R., Walker S.(1996). A review of Requirements for Simple Dispersion Models.

Building Research Establishment, Report No. CR77/96.

Hosker R.P.(1980). Flow and Diffusion Near Obstacles.

'Atmospheric Science and Power Production'. Ed D. Randerson. US Dept of Energy, DOE/CR-2521 (US Nuclear Regulatory Commission).

Shao L., Walker R.R., Woolliscroft M.(1993). Natural Ventilation Via Courtyards: Part II The Application of CFD.

14th AIVC Conference, 'Energy Impact of Ventilation and Air Infiltration'. Copenhagen, 21-23 September. pp235-250.

Walker R.R., Shao L., Woolliscroft M.(1993). Natural Ventilation Via Courtyards: part I - Theory and Measurements.

14th AIVC Conference, 'Energy Impact of Ventilation and Air Infiltration'. Copenhagen, 21-23 September. pp235-250.

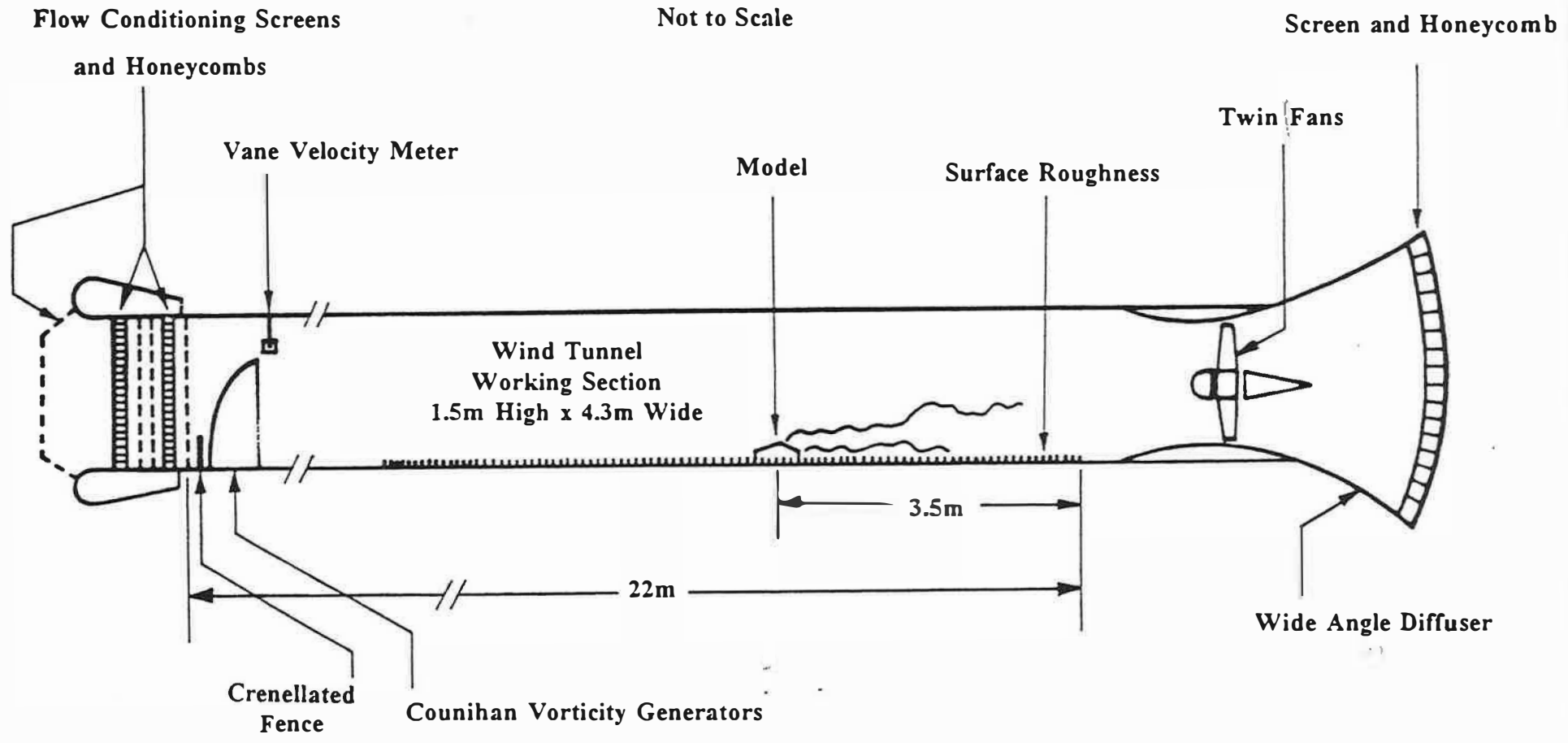


Figure 1. Diagram of Dispersion Modelling Wind Tunnel.

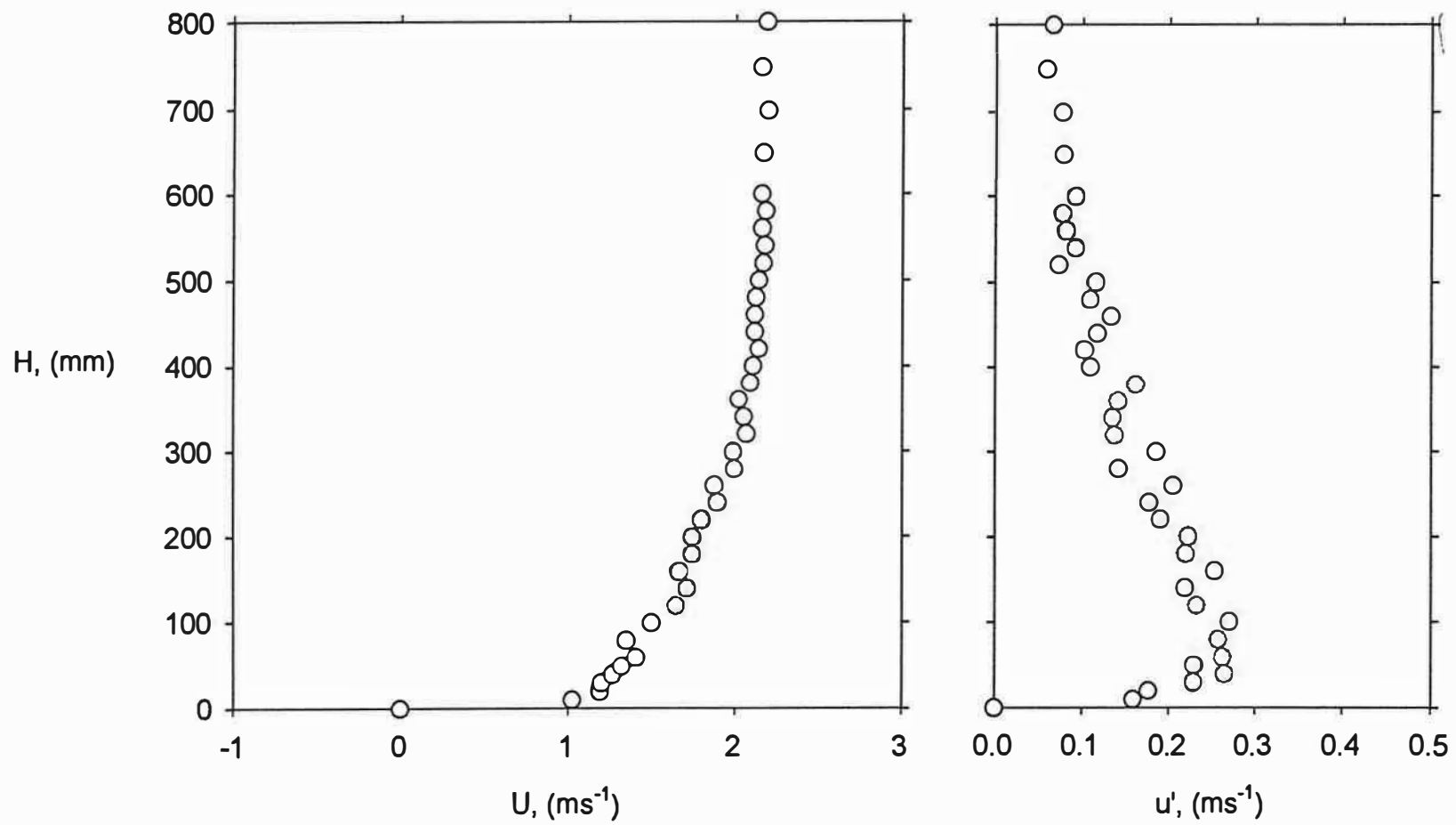


Figure 2. Wind Tunnel Boundary Layer - Velocity and Longitudinal Turbulence Profiles.

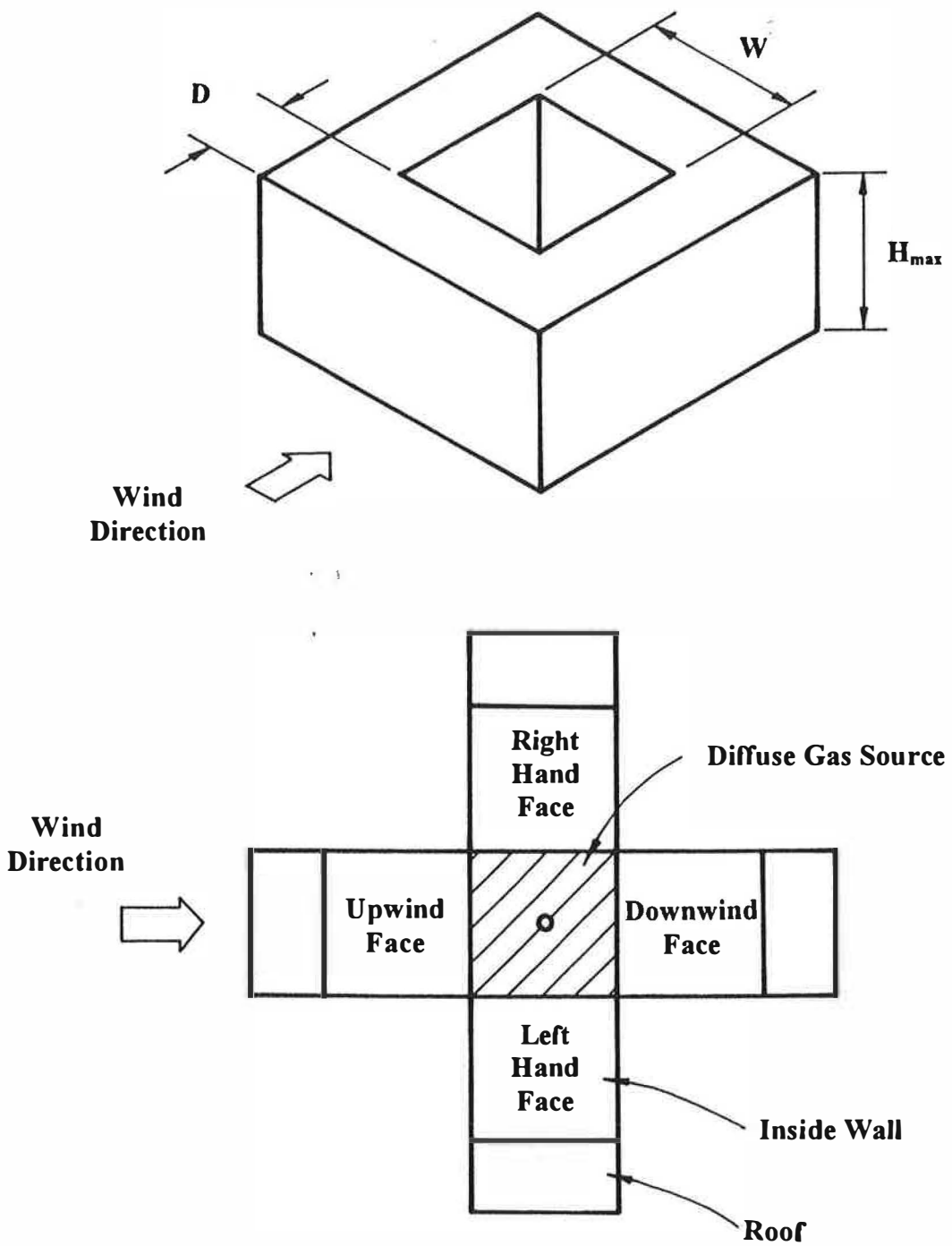


Figure 3. Diagram of Courtyard Showing Notation and Terminology.

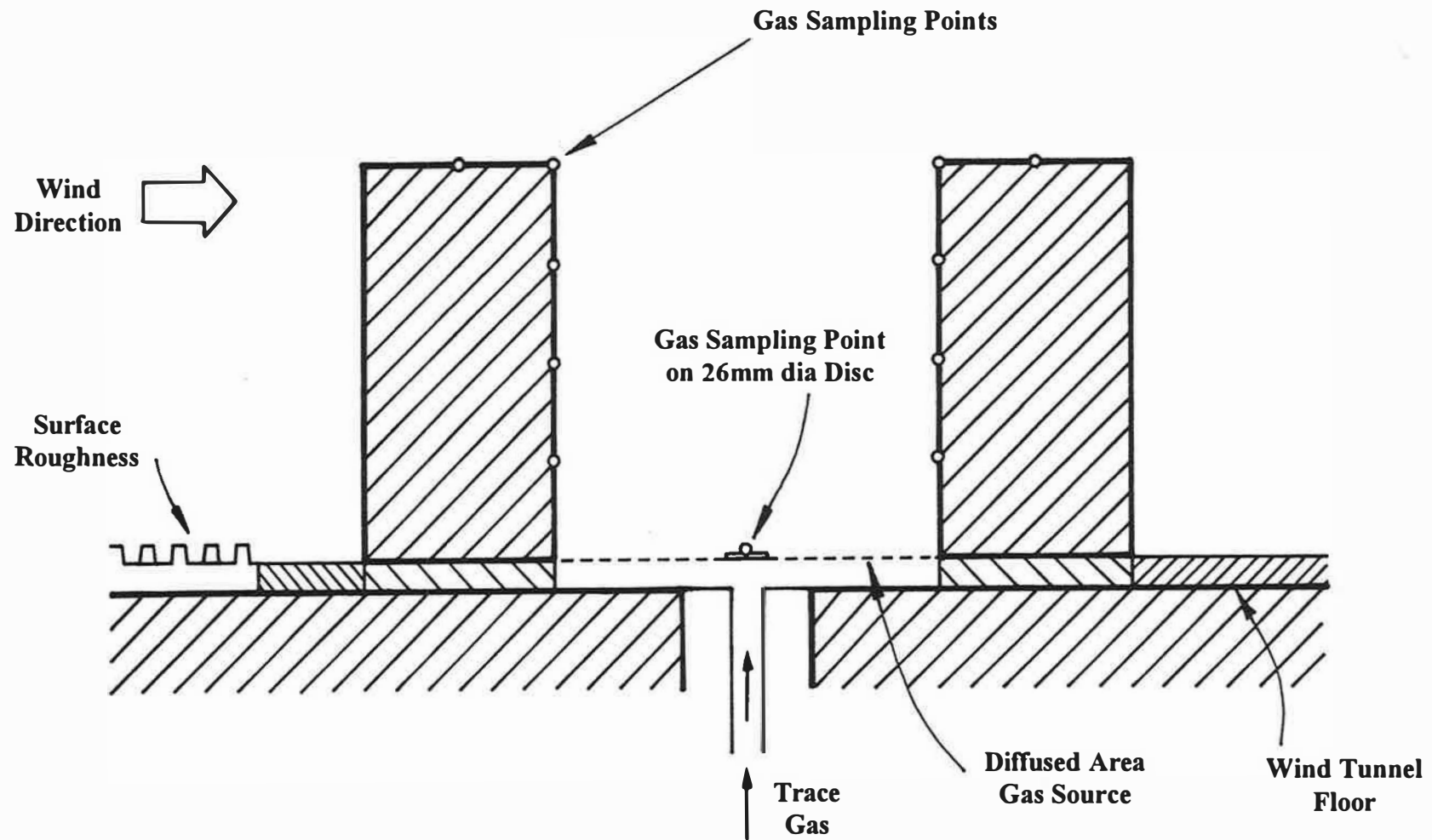


Figure 4. Diagram of a 'Courtyard' Set up in the Wind tunnel.

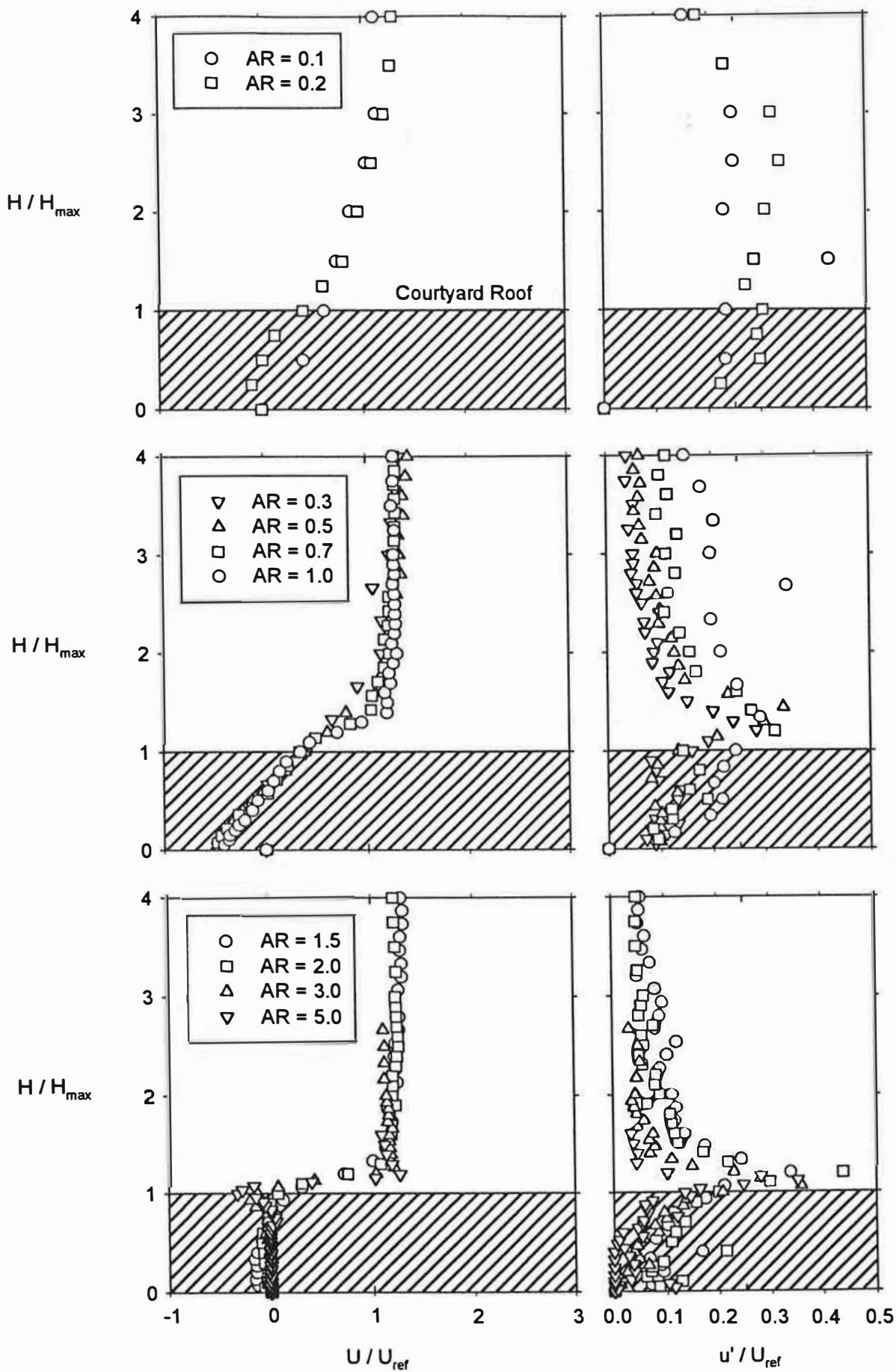


Figure 5. Velocity and Longitudinal Turbulence Intensity Profiles Through Centre of Courtyard. Courtyards of Varying Depth Set Normally to the Wind. Wind Direction 0° .

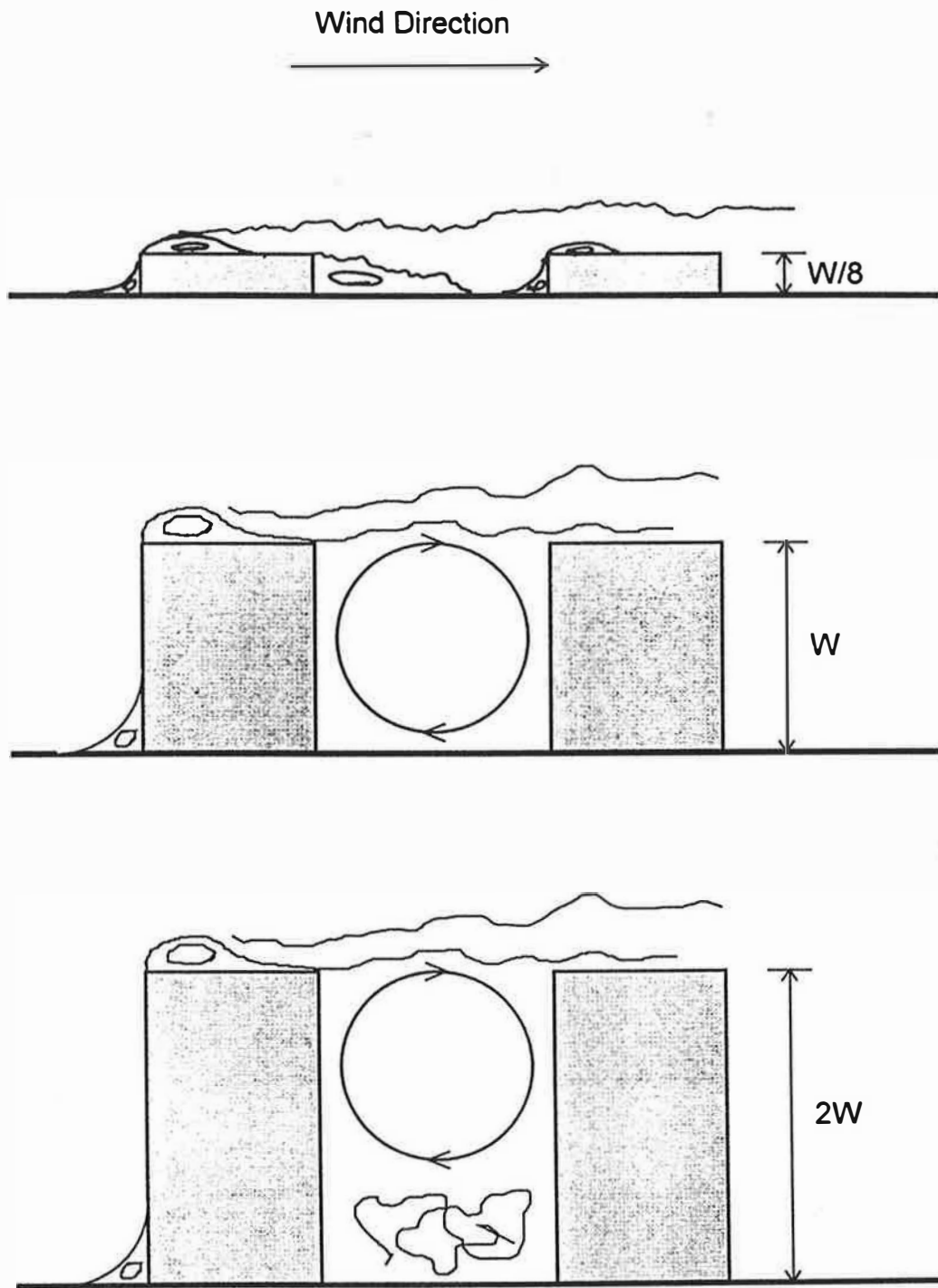


Figure 6. Sketches of the Three Types of Flow Patterns in Courtyards of Different Depth. The Sketches are not to Scale and the Separations Have Been Exaggerated.

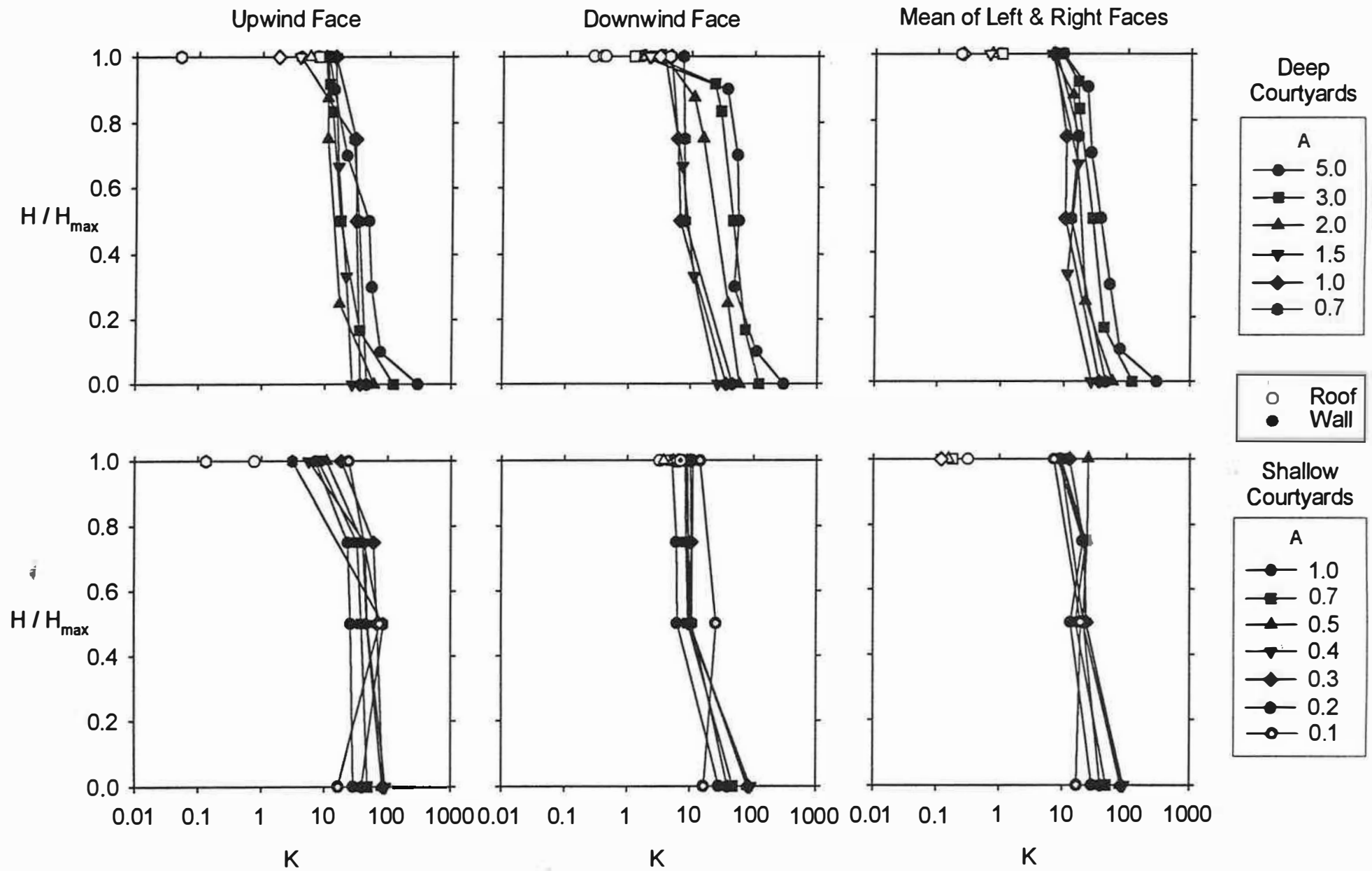


Figure 7. Vertical Concentration Profiles on Courtyard Walls. Courtyards of Varying Depth Set Normally to the Wind. Wind Direction 0° .

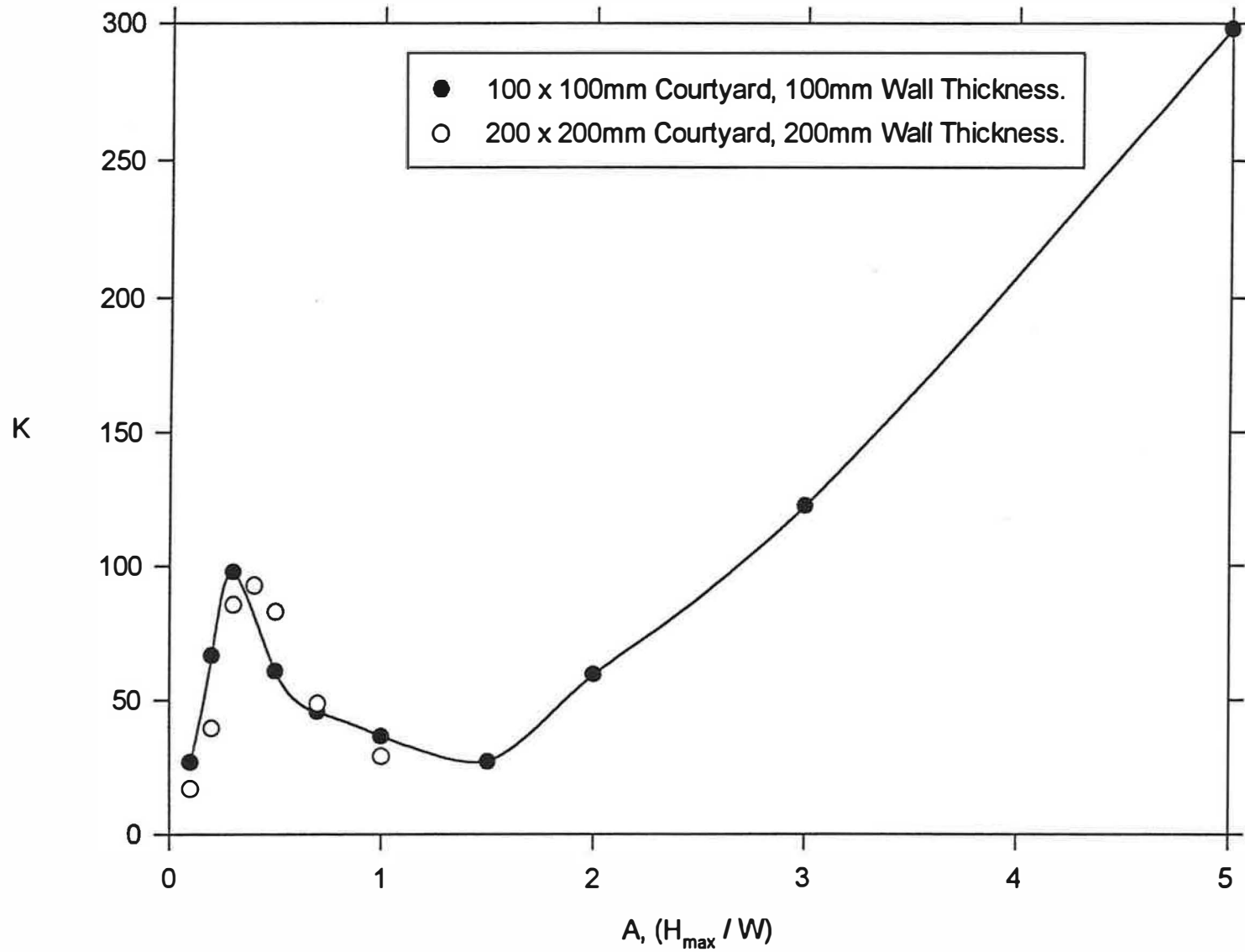


Figure 8. Effect of Aspect Ratio, H_{max}/W , on Concentrations at the Base of the Courtyard. Wind Direction 0° .

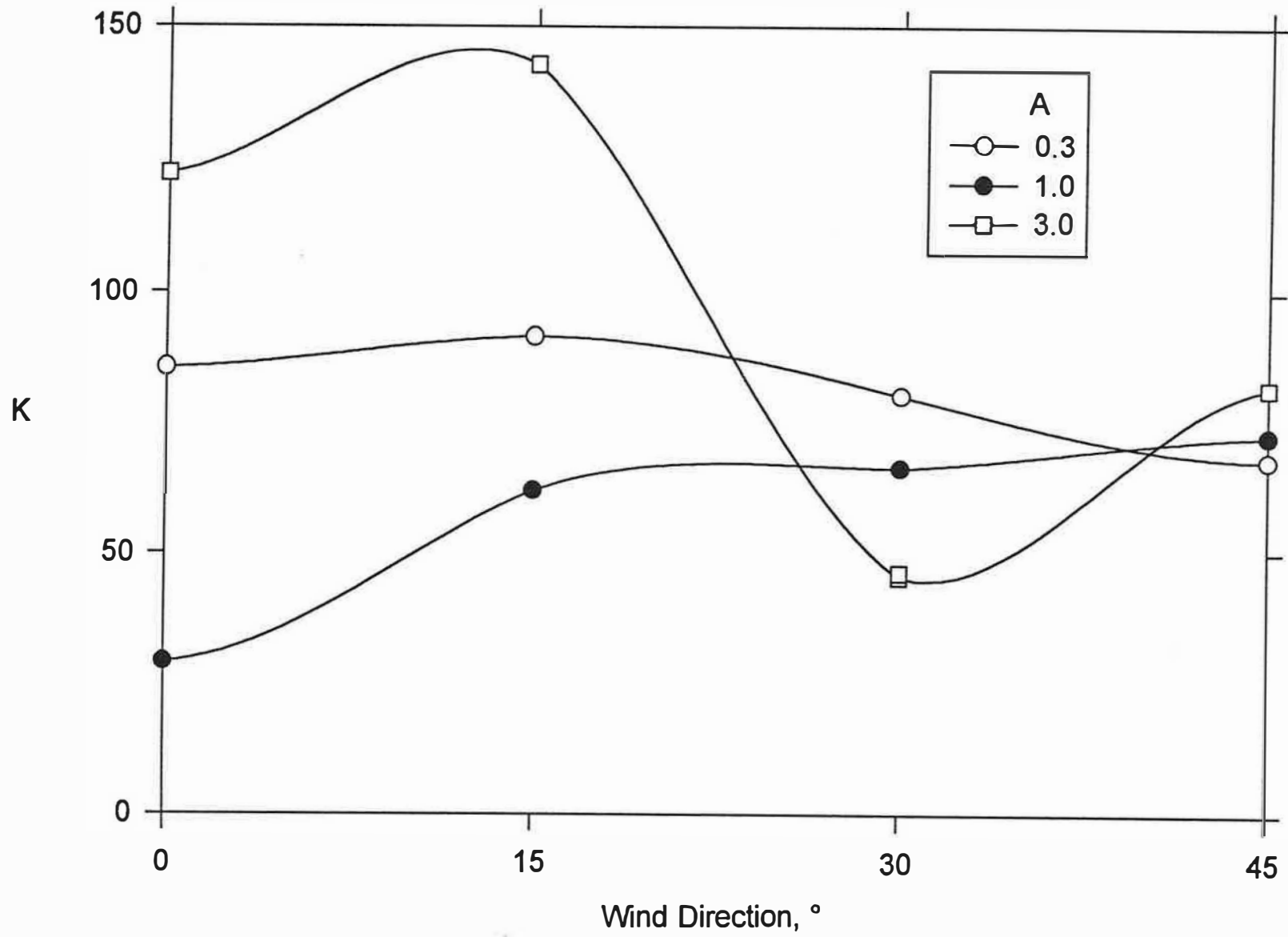


Figure 9. Effect of Wind Direction on Concentrations at the Base of the Courtyard.

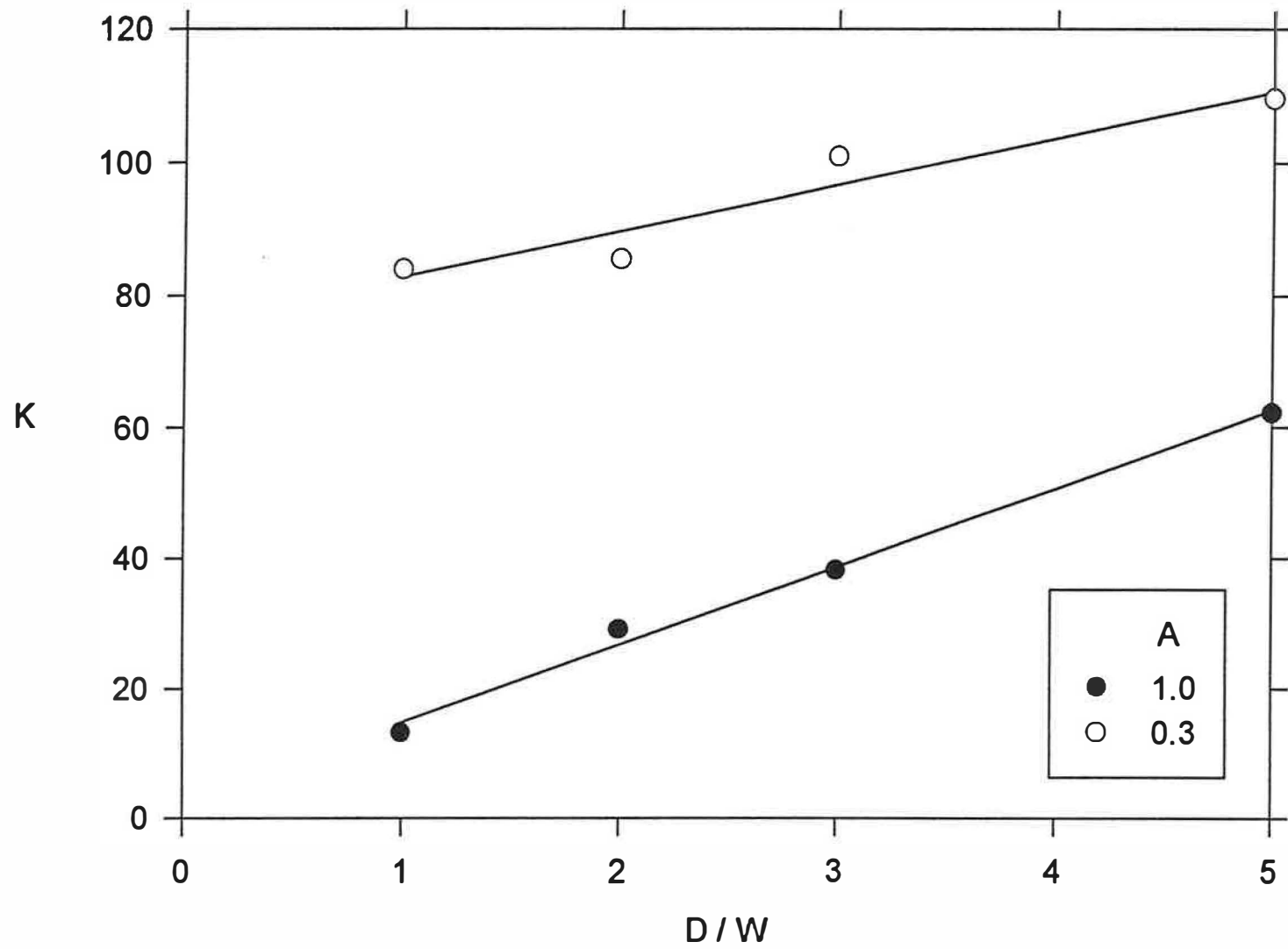


Figure 10. Effect of Wall Depth on Concentrations at the Base of the Courtyard.

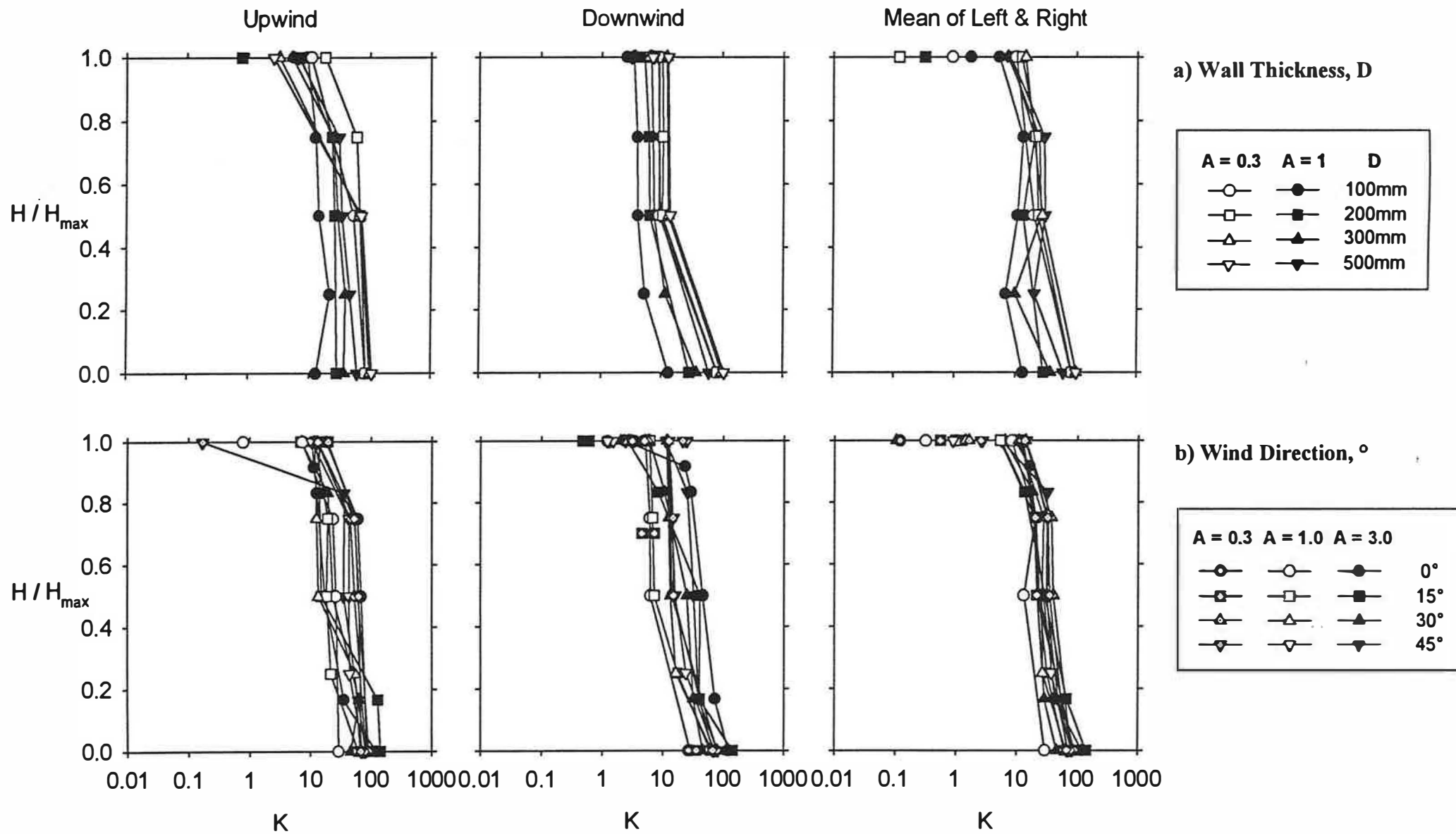


Figure 11. Vertical Concentration Profiles for Courtyards with Varying Wind Direction and Wall Thickness.

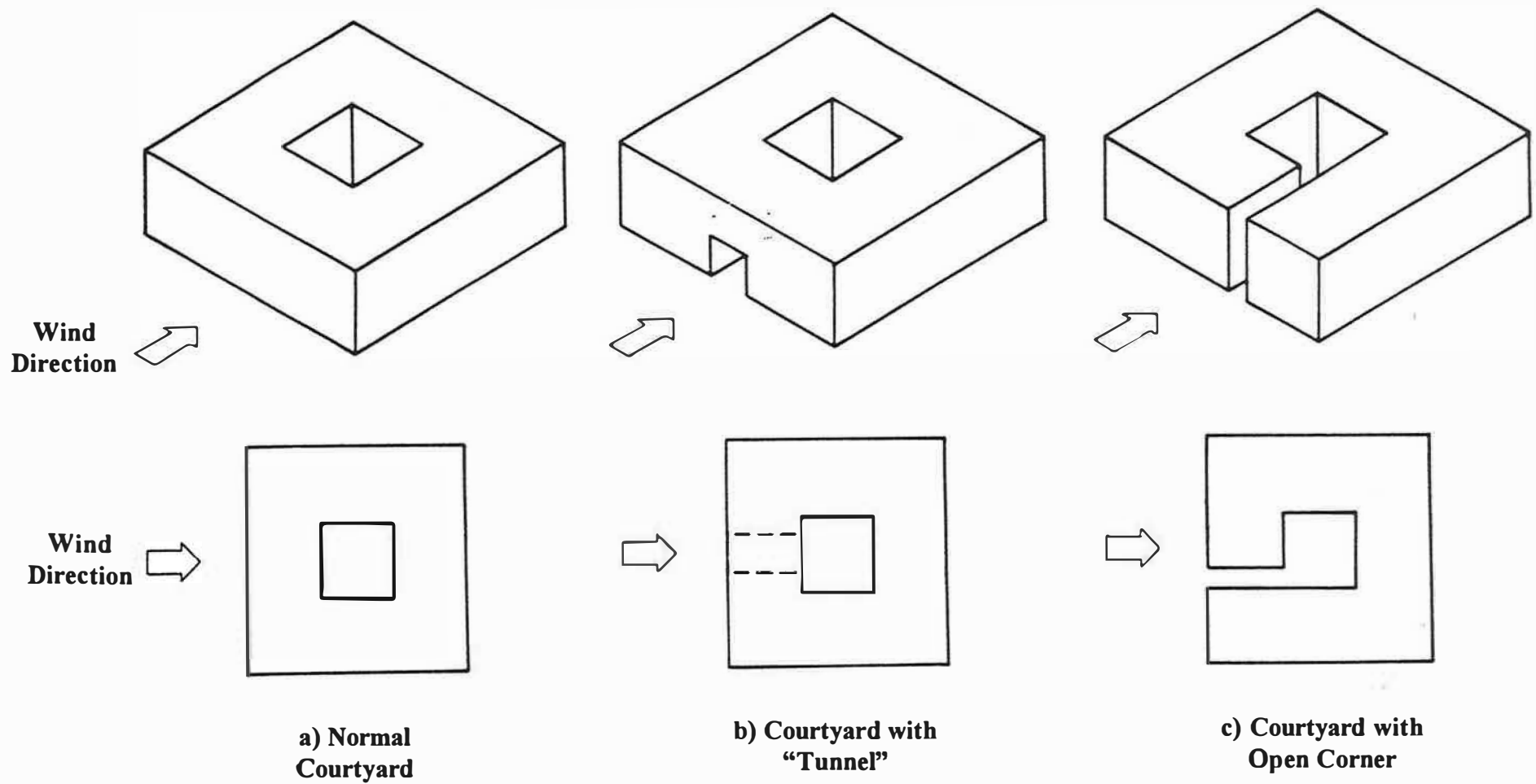


Figure 12. The Two Types of Courtyard with Openings Investigated. Both of Aspect Ratio 1.0.

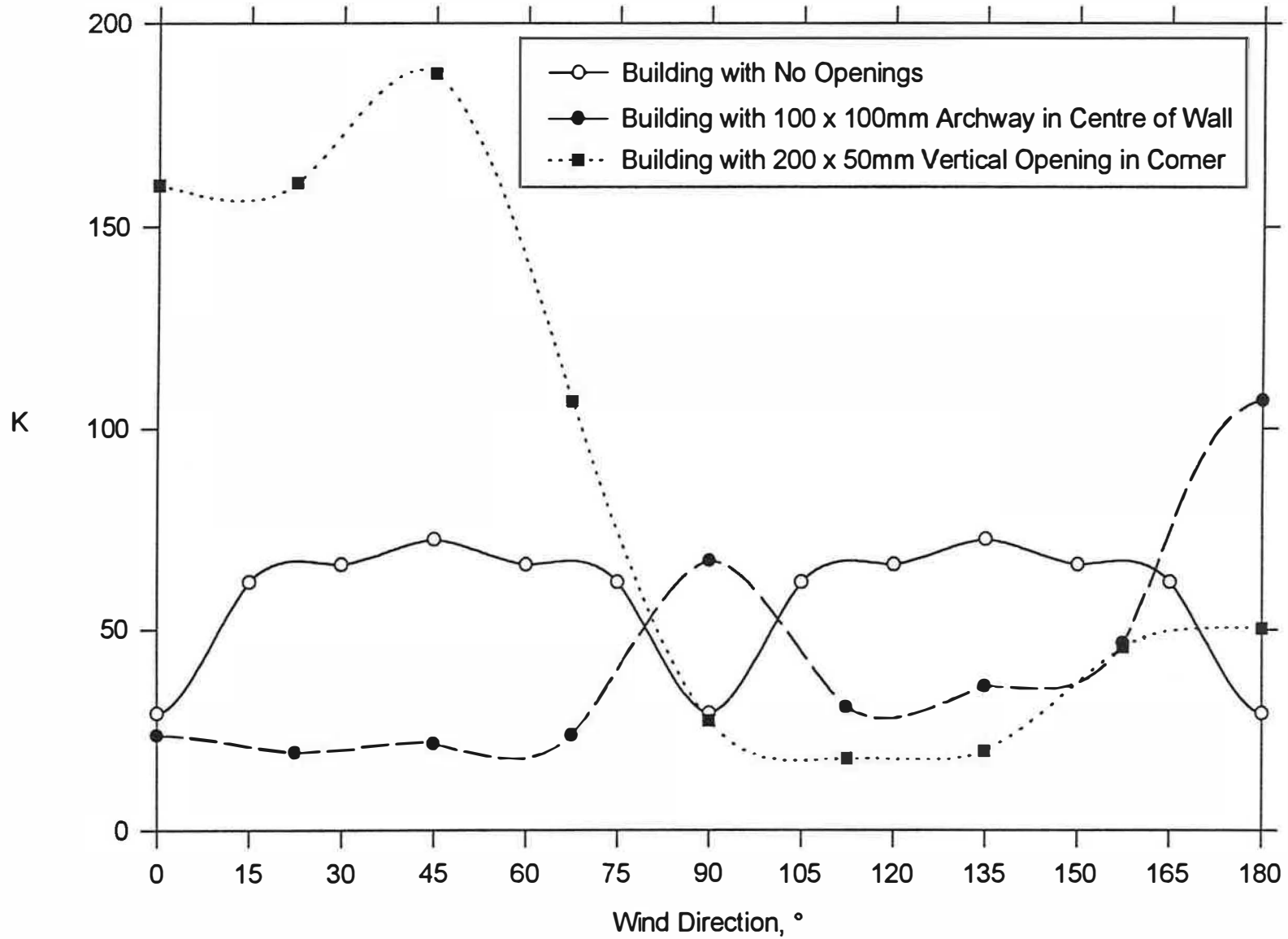
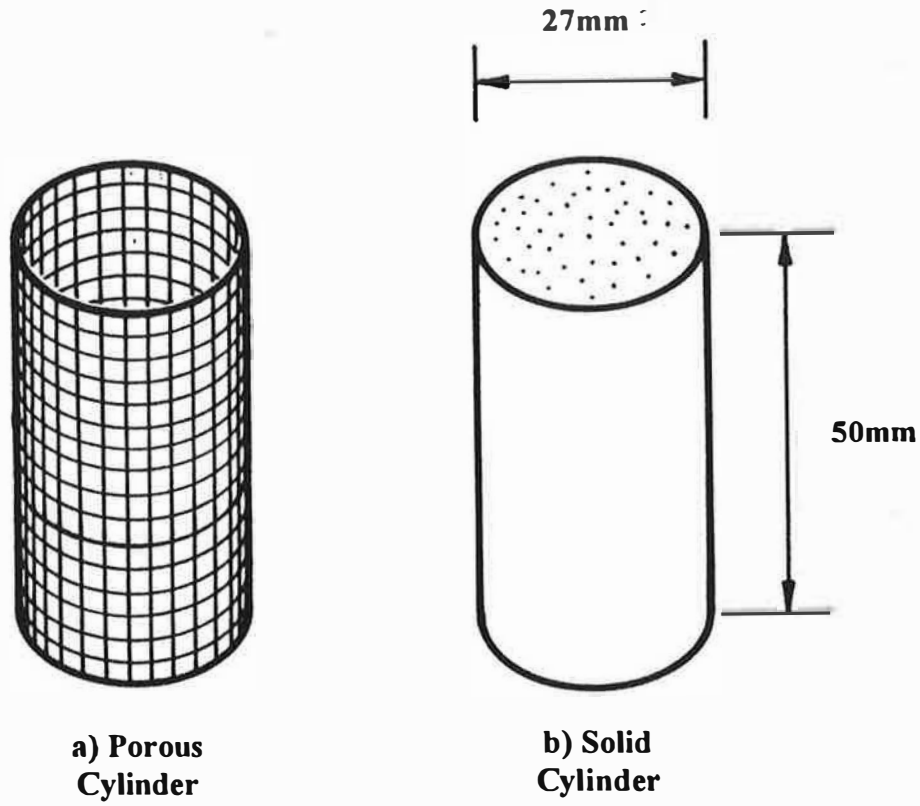
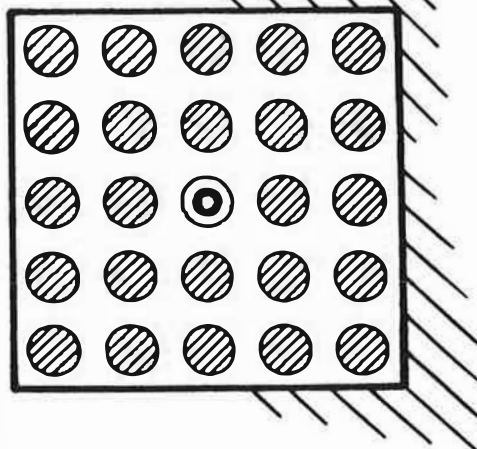


Figure 13. Concentrations at the Base of Courtyards with Openings, Showing the Effects of Wind Direction.



- ⊙ Gas Sampling Point
- ⊘ Surface Obstruction



c) Plan View of Surface Obstructions in Courtyard for 35% A_d

Figure 14. Types and Layout of Obstacles Used to Simulate Surface Clutter.

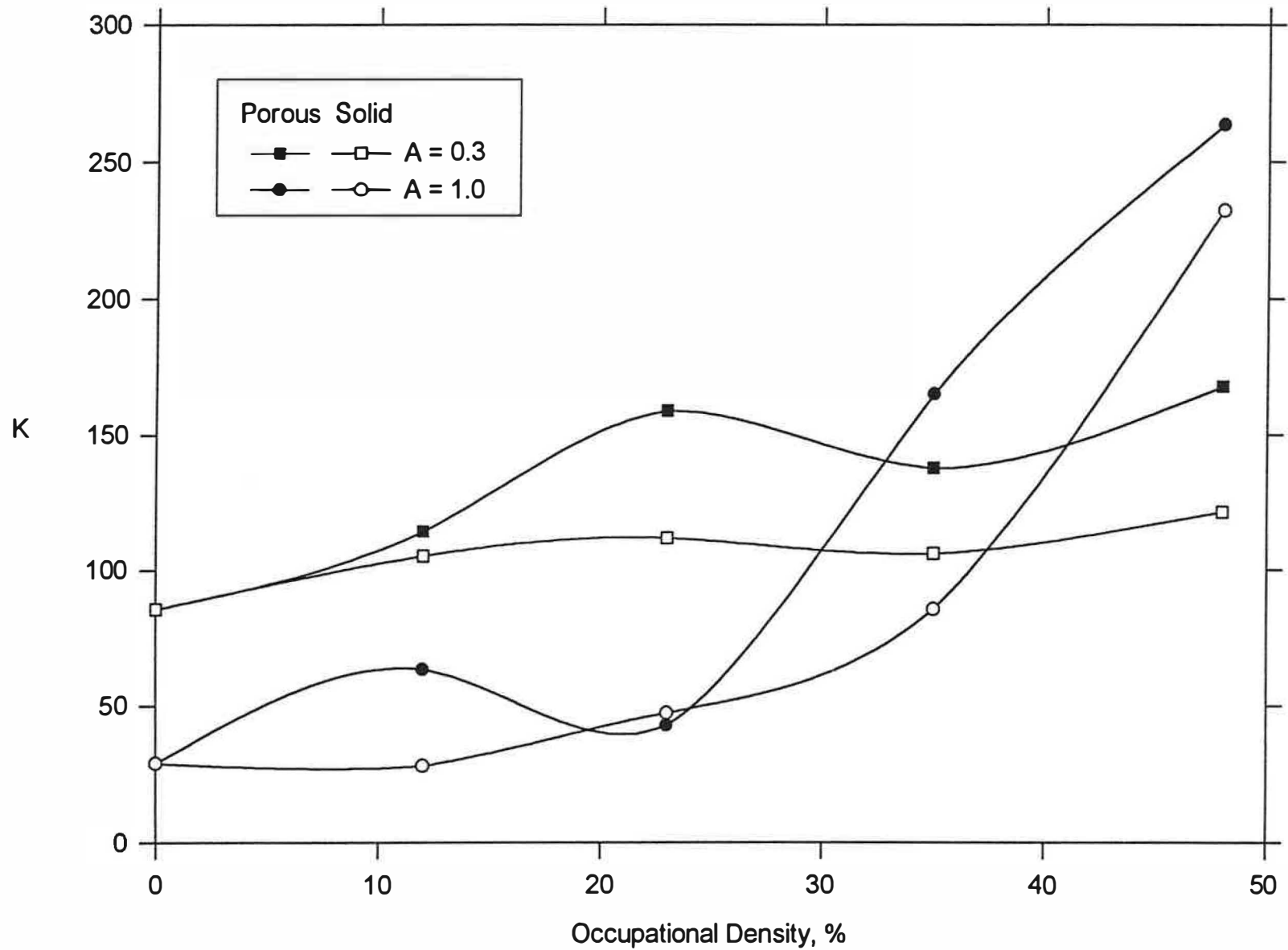


Figure 15. Concentrations at the Base of Courtyards with Surface Clutter.

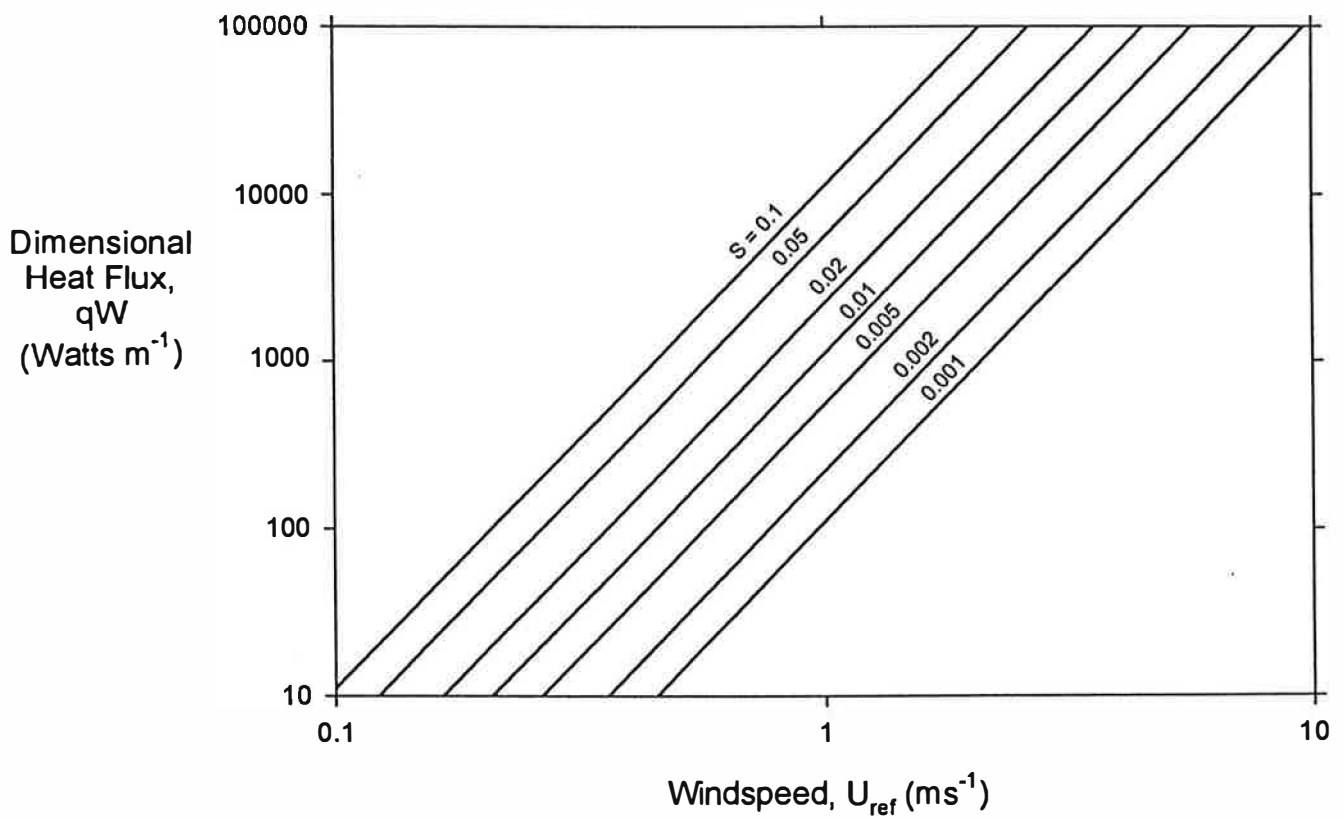


Figure 16. Values of the Stratification Parameter, S , Produced by Different Combinations of Courtyard Size, Windspeed and Surface Heat Flux. The Plot is Valid for Both Positive and Negative Heat Fluxes.

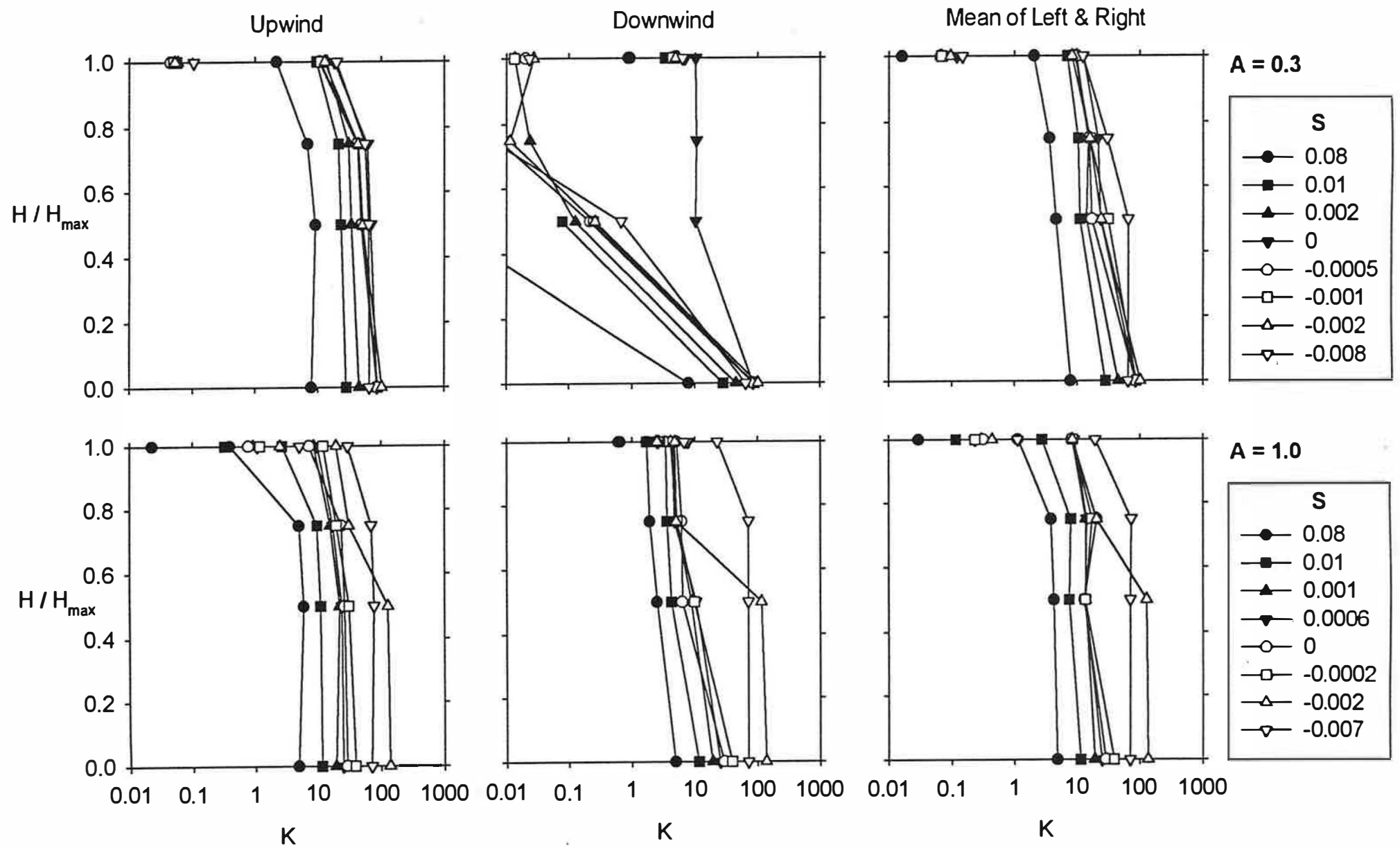


Figure 17. Vertical Concentration Profiles in Courtyards with Stratified Flows.

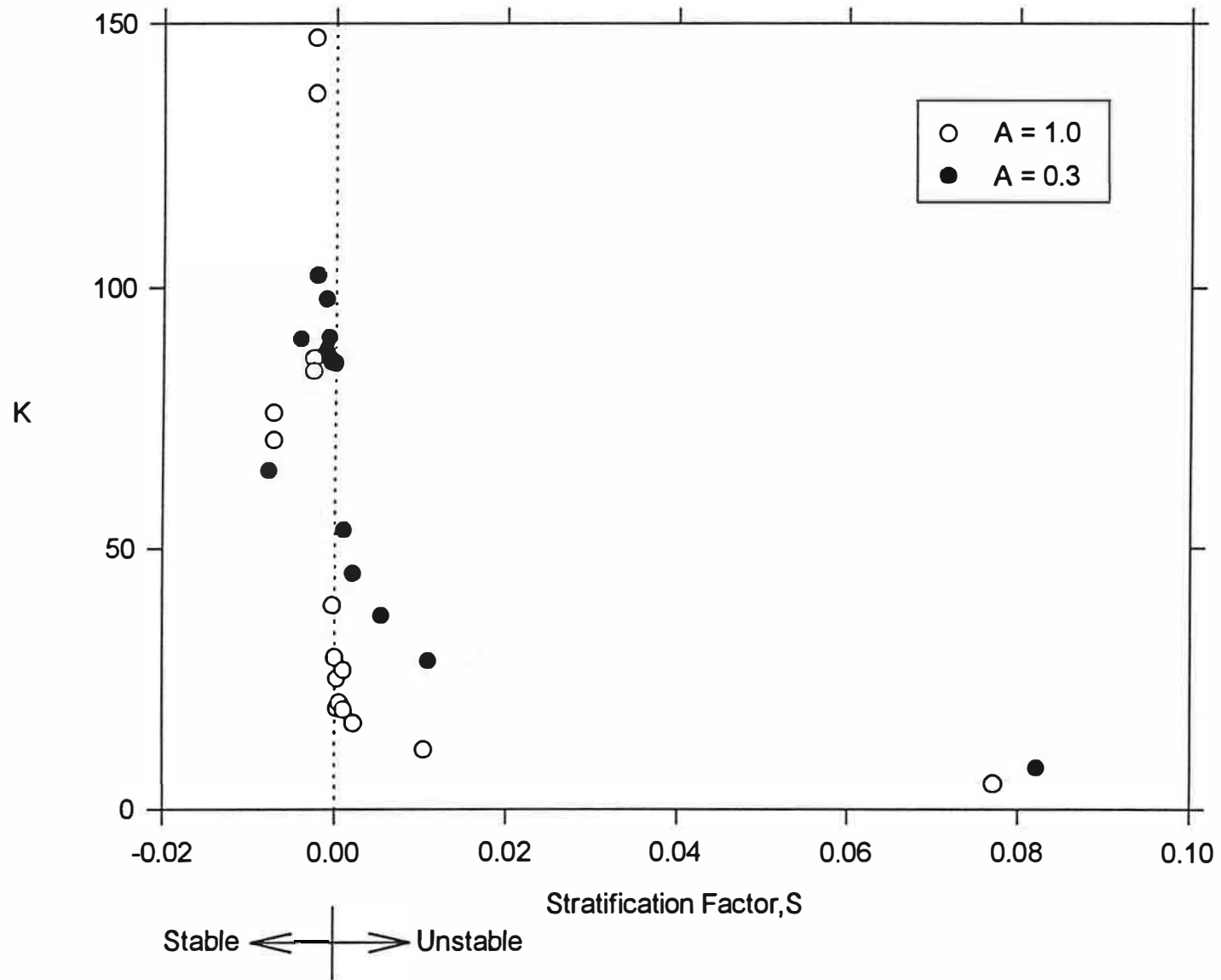


Figure 18. Concentrations at the Base of Courtyards with Stratified Flows.